Available online at www.sciencedirect.com
ScienceDirect
Deep-Sea Research II 53 (2006) 3116–3140
DEEP-SEA RESEARCH PART II
www.elsevier.com/locate/dsr2

Effects of variable winds on biological productivity on continental shelves in coastal upwelling systems

Louis W. Botsford[a,*], Cathryn A. Lawrence[a], Edward P. Dever[b], Alan Hastings[c], John Largier[d,c]

[a]*Department of Wildlife, Fish, and Conservation Biology, University of California, Davis, CA 95616, USA*
[b]*College of Oceanic and Atmospheric Sciences, Oregon State University, Corvallis, OR 97331-5503, USA*
[c]*Department of Environmental Science and Policy, University of California, Davis, CA 95616, USA*
[d]*Bodega Marine Laboratory, P.O. Box 247, Bodega Bay, CA 94923, USA*

Received 25 February 2005; accepted 7 July 2006

Abstract

The production and distribution of biological material in wind-driven coastal upwelling systems are of global importance, yet they remain poorly understood. Production is frequently presumed to be proportional to upwelling rate, yet high winds can lead to advective losses from continental shelves, where many species at higher trophic levels reside. An idealized mixed-layer conveyor (MLC) model of biological production from constant upwelling winds demonstrated previously that the amount of new production available to shelf species increased with upwelling at low winds, but declined at high winds [Botsford, L.W., Lawrence, C.A., Dever, E.P., Hastings, A., Largier, J., 2003. Wind strength and biological productivity in upwelling systems: an idealized study. Fisheries Oceanography 12, 245–259]. Here we analyze the response of this model to time-varying winds for parameter values and observed winds from the Wind Events and Shelf Transport (WEST) study region. We compare this response to the conventional view that the results of upwelling are proportional to upwelled volume. Most new production per volume upwelled available to shelf species occurs following rapid increases in shelf transit time due to decreases in wind (i.e. relaxations). However, on synoptic, event time-scales shelf production is positively correlated with upwelling rate. This is primarily due to the effect of synchronous periods of low values in these time series, paradoxically due to wind relaxations. On inter-annual time-scales, computing model production from wind forcing from 20 previous years shows that these synchronous periods of low values have little effect on correlations between upwelling and production. Comparison of model production from 20 years of wind data over a range of shelf widths shows that upwelling rate will predict biological production well only in locations where cross-shelf transit times are greater than the time required for phytoplankton or zooplankton production. For stronger mean winds (narrower shelves), annual production falls below the peak of constant wind prediction [Botsford et al., 2003. Wind strength and biological productivity in upwelling systems: an idealized study. Fisheries Oceanography 12, 245–259], then as winds increase further (shelves become narrower) production does not decline as steeply as the constant wind prediction.

Keywords: Upwelling; Primary productivity; Variable winds; Shelf production; Phytoplankton/zooplankton; Shelf fisheries

*Corresponding author.
E-mail address: lwbotsford@ucdavis.edu (L.W. Botsford).

0967-0645/$ - see front matter © 2006 Elsevier Ltd. All rights reserved.
doi:10.1016/j.dsr2.2006.07.011

1. Introduction

The importance of wind-driven coastal upwelling systems to global primary productivity and fishery production is well known. Upwelling areas on the continental shelf within eastern boundary currents contribute 20% of global fish production while occupying less than 1% of the world oceans' surface area (Ryther, 1969; Cushing, 1971; Mann, 2000). Production in upwelling areas varies from year-to-year and between locations, causing associated fisheries to vary, but the mechanisms underlying this variability are not well understood. For a variety of purposes, such as management of marine ecosystems and projection of the rates of global carbon fixation, it is important to understand the causes underlying spatial and temporal variability, and to establish indicators that allow for more accurate prediction of coastal productivity. A major goal of the present Wind Events and Shelf Transport (WEST) study, an observational and modeling study on the northern California coast, is to improve our understanding of the effects of wind variability on biological productivity over the shelf regions in coastal upwelling systems.

One of the primary questions in the WEST program regarding biological productivity has been how the positive effects of winds from upwelling of nutrient-rich water to the surface combine with the negative effects of horizontal advection of nutrients and biological production away from the area of original upwelling (e.g., off shelf) so that the potential production is not realized. In studies of fishery productivity on continental shelves, higher winds are commonly considered to lead to greater upwelling, hence greater production, while the fact that they can increase advective losses off the shelf is seldom considered. The advective removal of potential production represents a reduction of production available to the higher trophic levels in the shelf ecosystem. The shelf ecosystem is commonly of great biological and commercial importance. For example, in California it consists of a number of species of commercial importance (e.g., crabs, shrimp, prawns, many species of rockfish, several flatfish, and other fish) (Leet et al., 2001). In addition, there are a number of breeding colonies of seabirds on nearshore islands that feed on juveniles of fish species from this shelf ecosystem. In biological oceanographic studies of wind-driven production, the effects of off-shelf advection due to upwelling sometimes are included in models (e.g., Olivieri and Chavez, 2000), and there is a broad appreciation for the positive effects of occasional lulls in the wind (Send et al., 1987) on productivity (Wilkerson et al., 2006; Dugdale et al., 2006). Investigators typically focus on "optimal" patterns of upwelling winds, i.e. a period of upwelling to bring nutrient-rich waters to the surface, followed by a period of wind relaxation for the nutrients to be drawn down in the production of phytoplankton. There remains a basic scientific need to understand the consequences for production of *all* observed wind intensities and temporal patterns, and a practical need to describe how well they are represented by their standard indicator, upwelling rate.

The dominant indicator of productivity in upwelling systems over the past 30 years has been an estimate of volume upwelled computed from winds derived from atmospheric pressure fields (Bakun, 1973). Bakun's upwelling index has been empirically linked to fishery productivity in a number of species (Botsford and Wickham, 1975; Peterson, 1973; Nickelson, 1986; Botsford and Lawrence, 2002), but there have been few opportunities to assess its relationship to primary productivity (Thomas et al., 2003; Carr and Kearns, 2003; Ware and Thomson, 2005). This upwelling index is based on the premise that higher winds lead to a greater volume of nutrient-rich water upwelled, and that more nutrients will lead to higher production in proportion to that volume. In addition to this positive effect of winds and upwelling on nutrient supply, some comparative studies of upwelling systems have observed negative effects of strong winds on turbulence and transport of early life stages of fish and their prey off of continental shelves (Parrish et al., 1983; Ware, 1992). Some empirical characterizations of the dependence of biological productivity on upwelling winds have resulted in dome-shaped relationships (i.e. increasing then decreasing) between production and wind. For example, in the "optimal environmental window" of Cury and Roy (1989), the observed decline in productivity at higher winds was presumed to be due to increasing turbulence at higher winds (e.g., as in Lasker, 1975), though loss due to export off the shelf was also considered to be a possibility.

Previous modeling studies have also been used to improve our understanding of the observed effects of wind on productivity. Early modeling studies of upwelling focused on explaining the spatial structure of observed nutrient and phytoplankton

distributions (Walsh and Dugdale, 1971; Walsh, 1975). Wroblewski's (1977) two-dimensional (depth and distance offshore) model produced greater primary production at lower winds due to subductive losses at an offshore front in the resulting two-celled circulation. Using a similar slice configuration of a primitive equation circulation model, Spitz et al. (2003) examined the spatial distributions of plankton resulting from different ecosystem models and several time series of winds. In a companion paper, Newberger et al. (2003) approached the same issue by computing the temporal evolution of the spatial distribution of productivity across the shelf. Thus, while these modeling studies analyzed various aspects of the physical/biological processes involved in upwelling-driven productivity, they did not describe the general dynamic dependence of productivity on mean wind strength and temporal variability. This was due in part to the difficulty in applying analytical approaches to these complex models and to the computational demands of multiple model runs under various wind conditions.

Another modeling approach used recently is to formulate simpler, idealized models that focus on specific dynamic aspects of the physical/biological interactions underlying ecosystem responses to winds. Idealizations such as leaving out one or more spatial dimensions, or simplifying the physical dynamics allow for more comprehensive analyses of the specific dynamic mechanisms retained. There is a greater opportunity to employ analytical approaches and make extensive numerical simulations with less complex models. An example that focused on the effect of wind variability on upwelling productivity is the non-spatial (0-dimensional) model of Carr (1998). To study the effects of different time scales of winds on upwelling productivity, she used several versions of a Nutrient–Phytoplankton–Zooplankton (NPZ) model (Moloney and Field, 1991) with upwelling represented as the addition of nutrient-rich water containing no phytoplankton and zooplankton into the model. Models of other, non-coastal types of upwelling have represented its effects similarly (Hofmann and Ambler, 1988; Peña, 1994). The effect of upwelling in this formulation was to change the concentration of nutrients, phytoplankton and zooplankton from their current state to one more similar to newly upwelled water (i.e. higher nutrients, lower phytoplankton, lower zooplankton). Olivieri and Chavez (2000) approached the mechanism of offshore advective losses by using a non-spatial NPZ model with off-shelf advection of constituents equal to rate of volume upwelled. A limitation of these examples of simplified models is that they omit consideration of spatial aspects of upwelling production.

In our previous study of the effects of constant wind on productivity in coastal upwelling systems we formulated another simplified, idealized model, the mixed-layer conveyor (MLC) model, which follows the conventional conceptual view of upwelling as the transport of nutrient-rich water to the surface, then transport offshore as production takes place (Wilkerson and Dugdale, 1987; Mann, 2000; Botsford et al., 2003). This model focuses on the dynamics of the advective aspects of wind-driven upwelling, cross-shelf transport and advective losses from the shelf. Upwelling brings parcels of nutrient-rich water to the surface where drawdown begins, as an NPZ model describes development of phytoplankton, then zooplankton. Cumulative uptake of nutrients by phytoplankton, and phytoplankton by zooplankton, are computed up to the time that the parcel leaves the shelf. High upwelling rates lead to rapid transport across the shelf with the associated losses of material and forgone production. Analysis of this model for constant winds (Botsford et al., 2003) showed, as expected, that NPZ models corresponding to new production had a dome-shaped response to wind speed, with production increasing with upwelling volume up to the point that losses off the shelf began to dominate at high wind speeds. The value of shelf transit time at which that occurred could be determined graphically as the time corresponding to the point on a plot of cumulative phytoplankton or zooplankton development where a line through the origin was tangent.

Here we analyze the dynamic response of the MLC model to variable winds. We are interested in the effects of variability in winds on two different ecologically important time scales: the synoptic or event time scale and the annual time scale. We seek to understand their effects on the amount of new production available to shelf ecosystems. The model includes phytoplankton and zooplankton that are subject to passive offshore advection, but does not explicitly include higher trophic levels such as fish and invertebrates.

We frame this investigation as a comparison to the conventional view that the effects of upwelling are proportional to upwelled volume. This is a convenient null case for comparison for several reasons. First, if it were true, production would not

depend on the time scale of upwelling winds, just on the magnitude. Second, it is the most common interpretation of the effects of upwelling winds, as well as the most common basis for indices of upwelling in investigation of effects on biological production and fisheries (e.g., Bakun, 1973). We address the question, when does the integrated variability in volume upwelled accurately reflect biological productivity over the shelf? This builds on our previous study, which showed that for constant winds, upwelled volume accurately represented production up to a certain wind speed, beyond which production varied inversely with wind speed. In our assessment of inter-annual variability we also use this result as a null case for comparison, asking whether variable winds result in the same dependence on (seasonal means of) productivity on upwelling rate.

2. Model

The MLC model represents biological productivity in terms of the conveyor belt representation often used to illustrate coastal upwelling (e.g., Wilkerson and Dugdale, 1987; Mann, 2000; Botsford et al., 2003) (Fig. 1). Parcels of water are brought to the surface in response to wind, then transported offshore, while the nutrients in each are progressively converted to phytoplankton, then zooplankton. The dynamics of conversion of nutrients to phytoplankton, then to zooplankton, are represented by an NPZ model consisting of three nonlinear, coupled differential equations. We model productivity in terms of nitrogen, which we assume to be the limiting nutrient, e.g., Kudela and Dugdale (2000). Rate parameters for the single forms of phytoplankton and zooplankton are similar to those in Botsford et al. (2003). Rate parameters are chosen to represent rates of increase observed in WEST studies (Wilkerson et al., 2006). We do not include the shift-up effect (Zimmerman et al., 1987) in the basic model, but assess the influence of that effect in the discussion. The initial concentrations of nutrients (i.e. nitrate), phytoplankton and zooplankton in upwelled water are 17.5 mM, 2 mU and 0.5 mM, respectively, based on observations from WEST (Wilkerson et al., 2006). Values and units of all parameters for the NPZ

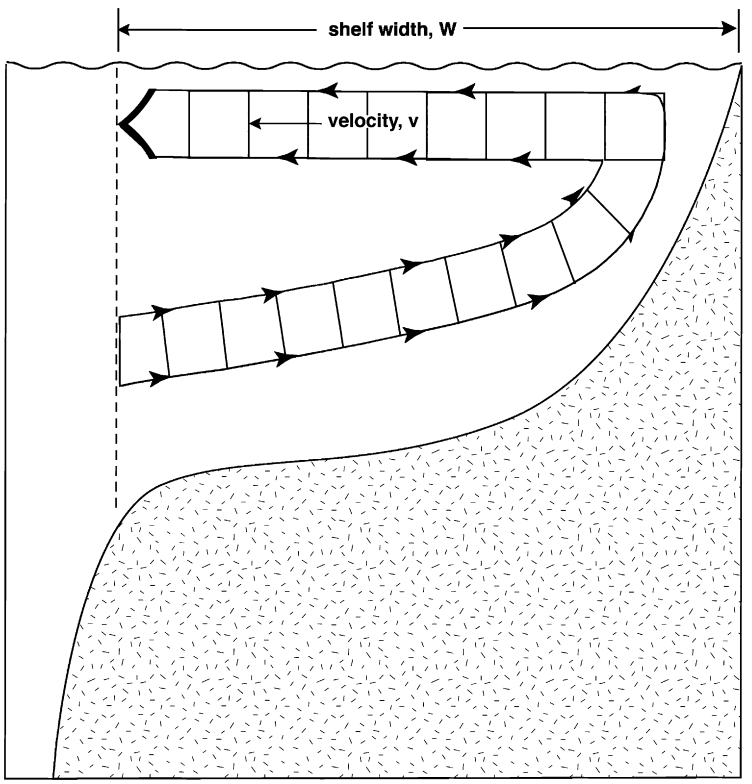

Fig. 1. A schematic view of the conceptual mixed-layer conveyor model portraying upwelling and shelf production as a two-dimensional flow across a continental shelf.

model are given in Table 1. Cross-shelf transport is calculated from the rate of cross-shelf Ekman transport and the depth of the mixed layer. The rates of shelf production for phytoplankton and zooplankton are taken to be the product of the velocity at which parcels are brought to the surface and advected offshore and the cumulative uptake per parcel up to the time that it leaves the shelf. Rate of production at time t is represented by

$$B(t) = v(t)F[T(t)], \tag{1}$$

where $v(t)$ is the cross-shelf velocity, $F[s]$ the cumulative production after time s at the surface, $T(t)$ the shelf transit time for a particle upwelled at time t.

The cross shelf velocity, $v(t)$, in Ekman transport is

$$v(t) = \frac{dx}{dt} = \frac{M_E}{D_{cst}}, \tag{2a}$$

where M_E is the Ekman mass transport and D_{cst} is the depth of the layer being transported offshore, here assumed to be the depth of the surface mixed-layer depth (MLD). M_E is related to alongshore wind stress by

$$M_E = \frac{\tau}{\rho f_c}, \tag{2b}$$

where ρ is the density of seawater, f_c is the Coriolis parameter and the magnitude of the wind stress, τ, is

$$\tau = \rho_a C_D V^2, \tag{2c}$$

where V is wind speed and ρ_a is density of air. Downwelling velocities are calculated, but downwelled volume is not subtracted when computing total upwelled volume. The wind-speed-dependent drag coefficient C_D was calculated as suggested by Trenbreth et al. (1990),

$$10^3 C_D = \begin{cases} 0.49 + 0.065V & \text{for } V > 10\,\mathrm{m\,s^{-1}}, \\ 1.14 & \text{for } 3\,\mathrm{ms^{-1}} \leqslant V \leqslant 10\,\mathrm{m\,s^{-1}}, \\ 0.62 + 1.5\,V^{-1} & \text{for } V < 3\,\mathrm{m\,s^{-1}}. \end{cases} \tag{2d}$$

Wind data for the model were taken from NDBC Buoy 46013 (hereafter referred to as buoy 13). Buoy 13 is located 28 km offshore of Bodega Bay, CA at 38.20°N, 123.30°W over the shelf at 125 m water depth. To represent wind forcing over the appropriate inertial time scale, the hourly data were low-pass filtered using PL64 which has a half-power point of 38 h (Beardsley et al., 1985).

The surface MLD is calculated from the regression relationship developed by Lentz (1992) for the Coastal Ocean Dynamics Experiment (CODE) study region, centered about 60 km north of the WEST study region:

$$\mathrm{MLD}_t = 6.2 + 0.7(h_{prt})_{t-8}. \tag{3a}$$

MLD_t is determined from h_{prt}, lagged by 8 h. This time lag and the 38-h filter applied to the wind data are assumed to provide a reasonable degree of offset between the surface wind forcing, the evolution of the surface mixed layer and of the development of offshore Ekman transport. The parameter h_{prt} developed by Pollard et al. (1973), is based on wind-generated shear at the base of the surface mixed layer and gives the wind-dependent scale of

Table 1
Symbol descriptions, parameter values and units for the NPZ model

Symbol	Symbol description	Value	Units
I	Irradiance	—	$\mu\mathrm{E\,m^{-2}\,s^{-1}}$
K_s	Half-saturation for P uptake of N	1.0	$\mu\mathrm{M\,N}$
N	Nutrient state variable	—	$\mu\mathrm{M\,N}$
P	Phytoplankton state variable	—	$\mu\mathrm{M\,N}$
R_m	Maximum ingestion rate of $P \times Z$	0.5	$\mathrm{day^{-1}}$
V_m	Maximum uptake rate of $N \times P$	1.0	$\mathrm{day^{-1}}$
Z	Zooplankton state variable	—	$\mu\mathrm{M\,N}$
g	Natural mortality rate of Z	0.2	$\mathrm{day^{-1}}$
k_P	Light extinction rate of P	0.016	$(\mu\mathrm{M\,P})^{-1}\,\mathrm{m^{-1}}$
k_W	Light extinction rate of seawater	0.06	$\mathrm{m^{-1}}$
m	Natural mortality rate of P	0.1	$\mathrm{day^{-1}}$
Λ	Grazing efficiency of Z on P	0.2	$(\mu\mathrm{M\,N})^{-1}$
γ	Assimilated fraction of P ingested by Z	0.7	Proportion
η	Regeneration rate of D–N	0.2	$\mathrm{day^{-1}}$

Parameter values are those of Franks and Walstad (1997).

the depth of the surface mixed layer. The values of the coefficient A, the density of seawater, ρ, and the buoyancy frequency, N_I, are assumed to be constant.

$$h_{\mathrm{prt}} = A\sqrt{\frac{|\tau|}{\rho f_{\mathrm{c}} N_I}}. \tag{3b}$$

The expressions for cumulative production, F, (Eq. (1)) differ for phytoplankton and zooplankton. They are based on a simple ecosystem model for nutrients, N, phytoplankton, P, and zooplankton, Z:

$$\frac{\mathrm{d}N}{\mathrm{d}t} = -\frac{V_{\mathrm{m}}N}{K_{\mathrm{s}}+N} f(I)P, \tag{4a}$$

$$\frac{\mathrm{d}P}{\mathrm{d}t} = \frac{V_{\mathrm{m}}N}{K_{\mathrm{s}}+N} f(I)P - mP - R_{\mathrm{m}}(1-\mathrm{e}^{-\Lambda P})Z \tag{4b}$$

and

$$\frac{\mathrm{d}Z}{\mathrm{d}t} = \gamma R_{\mathrm{m}}(1-\mathrm{e}^{-\Lambda P})Z - gZ, \tag{4c}$$

where the definition of variables is in Table 1. This model represents new production. It is the model developed by Franks and Walstad (1997) with the feedback paths from zooplankton and phytoplankton to nutrients removed. This was done to remove the inherent instability in the close coupling of regenerated production when a parabolic mortality rate, time delays or diffusion are not included (Edwards et al., 2000; Newberger et al., 2003; Botsford et al., 2003). The model was parameterized to produce the magnitudes and time scales of productivity observed during WEST (Wilkerson et al., 2006).

The functions represented by F in Eq. (1) are the cumulative uptake of nutrients by phytoplankton, F_P, and the cumulative consumption of phytoplankton by zooplankton, F_Z. These are:

$$F_P(T) = \int_0^T \frac{V_{\mathrm{m}}N}{K_{\mathrm{s}}+N} f(I)P\,\mathrm{d}t \tag{5a}$$

and

$$F_Z(T) = \int_0^T \gamma R_{\mathrm{m}}(1-\mathrm{e}^{\Lambda P})Z\,\mathrm{d}t, \tag{5b}$$

where the integrands are the first terms in Eqs. (4b) and (4c), respectively, in the ecosystem models in Eq. (3). $F_P(T)$ is the total gross phytoplankton production in a parcel when it reaches the shelf edge, ignoring losses due to mortality and zooplankton consumption. $F_Z(T)$ is the total gross zooplankton production in a parcel when it reaches the shelf edge, ignoring zooplankton mortality. Both of these depend on the initial nutrient concentration and light level. The influence of light extinction by seawater and phytoplankton (Bannister, 1974)

$$I_z = I_0\mathrm{e}^{-(k_{\mathrm{w}}+k_P P)z} \tag{6a}$$

is averaged over the assumed MLD. As such, the mixed layer average light, including self-shading by the phytoplankton, is computed from surface light intensity (I_0)

$$\bar{I} = \frac{1}{\mathrm{MLD}}\int_0^{\mathrm{MLD}} I_0\mathrm{e}^{-(k_{\mathrm{w}}+k_P P)}, \tag{6b}$$

which is

$$\bar{I} = \frac{I_0}{\mathrm{MLD}(k_{\mathrm{w}}+k_P P)}\left(1-\mathrm{e}^{-(k_{\mathrm{w}}+k_P P)\mathrm{MLD}}\right), \tag{6c}$$

and the light level influences phytoplankton growth according to

$$f(\bar{I}) = 1-\mathrm{e}^{-0.006\bar{I}}. \tag{6d}$$

We assumed a MLD of 17 m for the NPZ model in spite of the τ-dependent MLD used to calculate of cross-shelf velocity (described above). This was an extension of our previous work (Botsford et al., 2003) in which a constant MLD of 17 m was used for both. A MLD of 17 m is typical for the WEST study region during upwelling favorable wind conditions (Lentz, 1992; Dever et al., 2006). We tested the sensitivity of our results to the assumption of a constant MLD for the NPZ model by simulating a more computationally intensive model. The results (described below) indicate little difference between the assumed model and the more realistic version. The value of T in Eq. (1) is the time increment required for a particle upwelled at time t to cross a shelf of width W. It is given implicitly by

$$\int_t^{t+T} v(\tau)\,\mathrm{d}\tau = W. \tag{7}$$

3. Example of time series

Plots of time series of the elements of Eq. (3) versus time for 2001 illustrate the nonlinear mechanisms involved in the production of phytoplankton and zooplankton in the context of this model (Fig. 2). The cross-shelf velocity (Fig. 2A) reflects rather high upwelling during

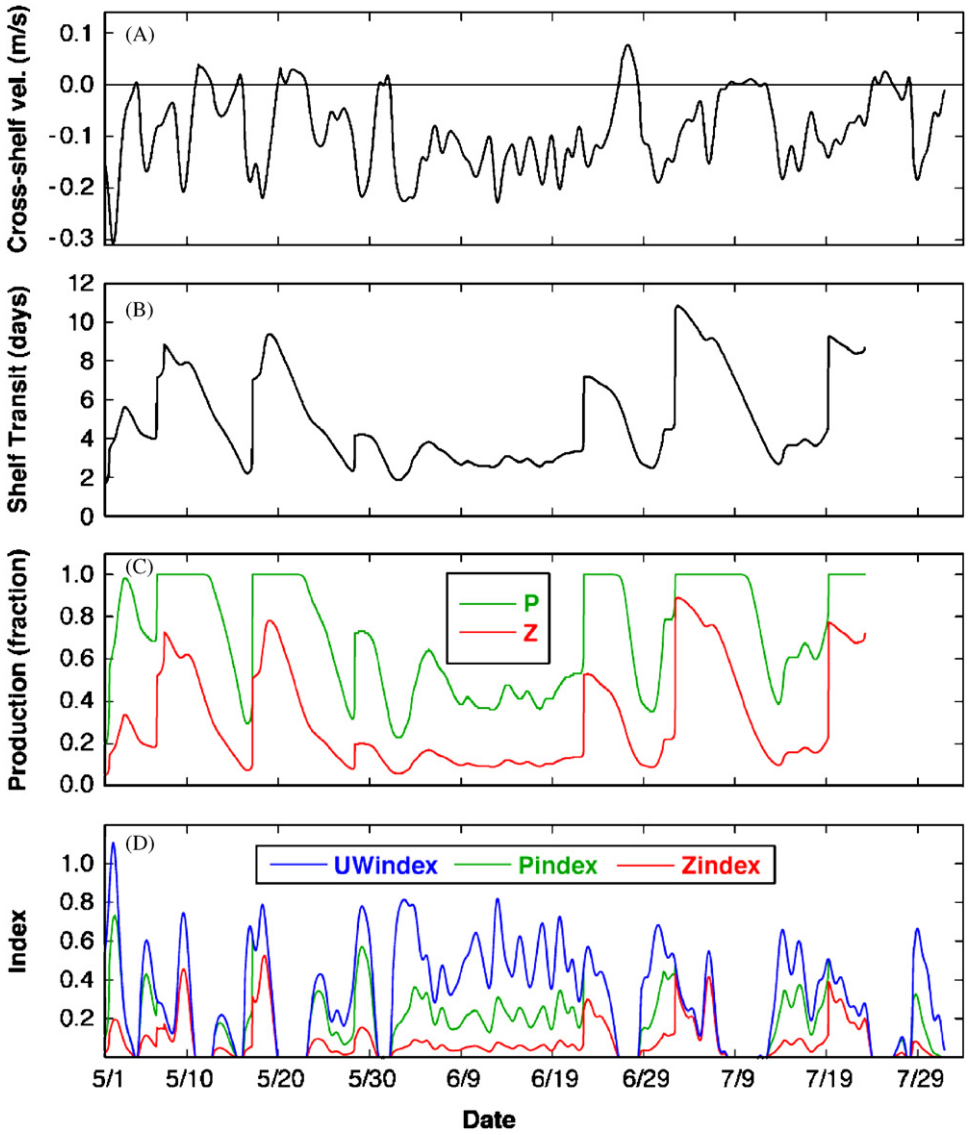

Fig. 2. MLC model example using NDBC Buoy 13 winds for 2001 and a shelf width of 35 km. (A) Cross-shelf velocity at each time (negative values represent the offshore direction), (B) the time required for a parcel upwelled at time t to transit the shelf, (C) fraction of maximum possible production of phytoplankton (green) and zooplankton (red) that would be produced in a parcel if it were upwelled at time t, by the time it reached the edge of the shelf, (D) volume upwelled at each time t (UWindex, blue), and the resulting amount of phytoplankton (Pindex, green) and zooplankton (Zindex, red) produced. Pindex and Zindex are the product of the fraction of maximum production (Fig. 1C) and UWindex. The units of UWindex are 10^2 km.

May, punctuated by occasional reversals. That is followed in early June by a period of moderate upwelling with no relaxations through June 25, after which relaxations occur occasionally.

A salient feature of the plot of parcel-specific shelf transit times (Fig. 2B) is the jumps to high values followed by gradual declines. A substantial part of the production of both phytoplankton and zooplankton per upwelled parcel occurred in these parcels with long transit times (Fig. 2C and D). To understand why these occur, we expanded the time scale in Fig. 3A. The definition of T (Eq. (7)) as the time taken for integrated velocity to move the particle a distance W corresponds to examining the integral of velocity to determine how long it takes to increase by 35 km at each point (i.e. to move across the shelf (Fig. 3B). In this plot, for each time, one moves vertically a distance equal to the shelf width

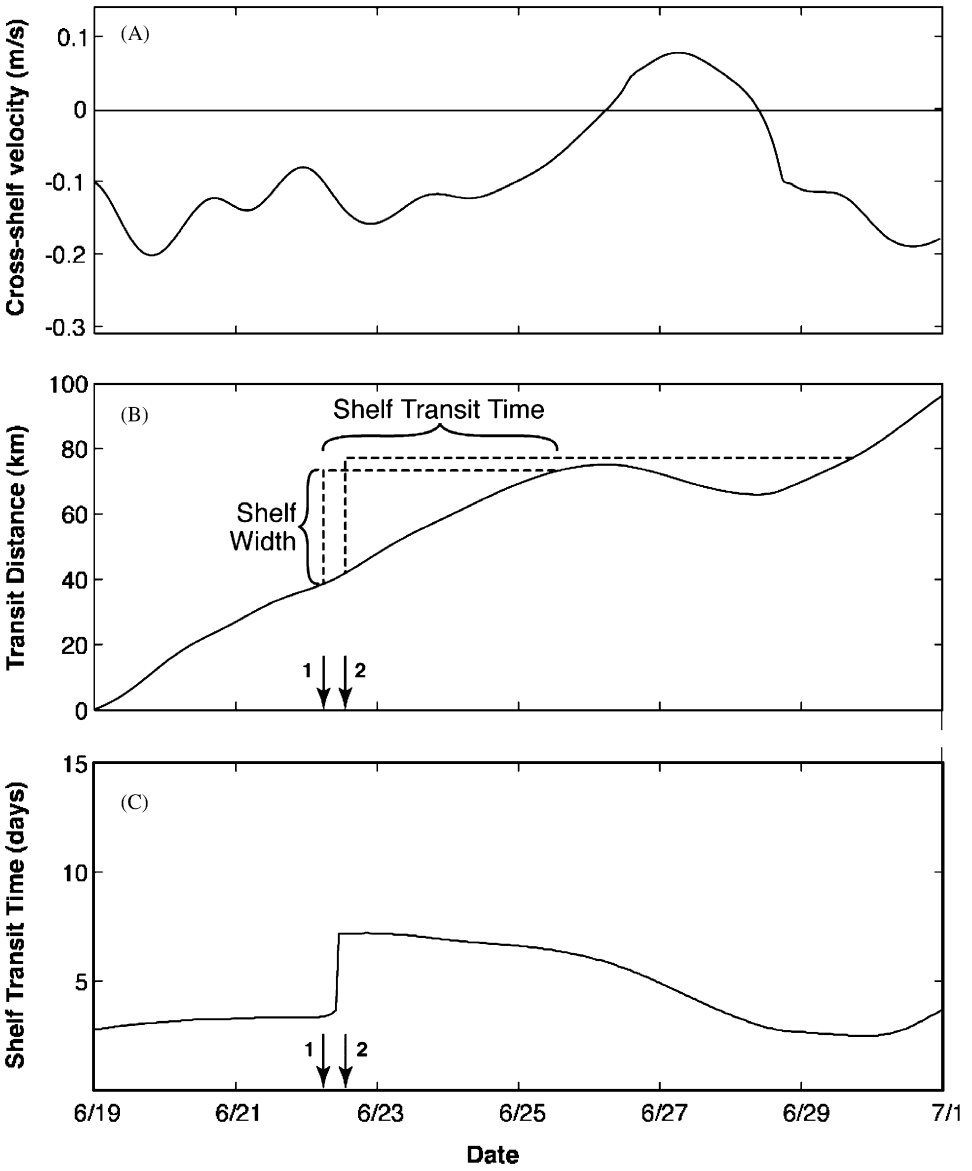

Fig. 3. Illustration of the mechanism underlying the jumps in shelf transit time in Fig. 1 from 6/19 to 7/1: (A) cross-shelf transit time (from Fig. 1A with expanded time scale), (B) the cumulative distance moved by an upwelled particle over this time period shown so that the time required to travel a distance equal to the shelf width by a particle upwelled at each time can be identified (e.g., the horizontal dashed lines corresponding to parcels upwelled at times 1 and 2), and (C) the resulting values of shelf transit time. Between times 1 and 2, the length of the horizontal dashed line in (B) (i.e., the shelf transit time) jumps from about 3 days to about 7 days, and that is plotted in (C).

above the line in Fig. 3B, then measures the horizontal distance to the right to determine the time required to move that distance. When a brief reversal occurs, as it did on about June 27, there is a dip in the integral of velocity (Fig. 3B). That causes the time required to travel a distance equal to the shelf width to jump across that dip, causing a positive jump in the transit time (Fig. 3C). Following this mechanism we can see that the rapid increases in shelf transit time (Fig. 2B) for parcels upwelled on May 5, 17, June 23, July 2 and 19 were caused by relaxations (Fig. 2A) on May 11–12, 21–23, June 26–28, July 8–10 and 24–25, respectively.

Production per parcel of both phytoplankton and zooplankton is determined by the shelf transit time of the particle (Fig. 2B) and the time course of cumulative production (Fig. 4). The time courses of

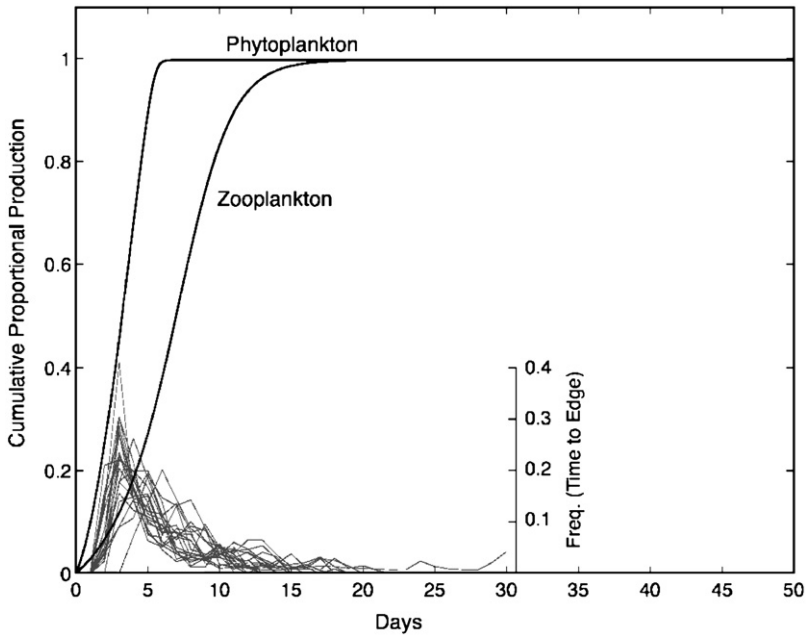

Fig. 4. The maximum potential new production, (i.e. model's cumulative increase in phytoplankton and zooplankton) in a parcel of upwelled water as it travels across the shelf is shown along with distributions of cross-shelf transport time computed from Eqs. (2) and (7) and NDBC Buoy 13 winds over the past 20 years and the local WEST shelf width of 35 km.

phytoplankton and zooplankton production per parcel illustrate that it requires 5 days for phytoplankton to reach maximal new production rates and 9.6 days for zooplankton to completely consume the phytoplankton. (We define these times in terms of the break point between increasing and decreasing dependence on constant wind, i.e. the point at which a line through the origin in Fig. 3 is tangent to the cumulative production (Botsford et al., 2003).) From Fig. 2C, one sees that the time course of conversion of nutrients to phytoplankton and phytoplankton to zooplankton approaches completion only in parcels beginning at and just following the jumps in transit time. Conversion of phytoplankton to zooplankton reaches completion for fewer particles, consistent with the longer time required.

The ultimate resulting new production is the product of upwelling per parcel and upwelling rate (Fig. 2D). The central question of whether upwelled volume adequately predicts new production is essentially whether the green (phytoplankton) or red (zooplankton) closely resemble the blue line in Fig. 2D (i.e. how important is the variability in Fig. 2C?). We address that question below for the synoptic time scale shown here, as well as the inter-annual time scale, which would involve averages over the upwelling seasons (several months).

It is informative to relate the plots in Fig. 2 to the observations from the cruise in 2001 and the instruments on the moorings. The broad-scale cruises following the upwelling period ending on May 19 indicate a cool, saline upwelling tongue from the Pt. Arena upwelling area in the northern part of the WEST area, and nitrate decreasing from north to south along what can be viewed as the transport path of the MLC model (Fig. 8 in Wilkerson et al., 2006). The time series of samples indicates a decline in nitrate from May 19th through May 24th as chlorophyll increases from just detectable levels to a maximum on May 25th (Fig. 10B and C in Wilkerson et al., 2006). This event can also be seen in Fig. 2, in the time series of shelf transit time (Fig. 2B), production per parcel (Fig. 2C) and actual production (production per parcel times upwelling rate, Fig. 2D), all indexed by the time at which a parcel is upwelled. Note that the relaxation from May 21 to 25 leads to a reduction in cross-shelf velocity (Fig. 2A), which increases the transport time of parcels upwelled from about May 18 to 24 (Fig. 2B). That would lead to high phytoplankton production in any parcel upwelled over that same period (Fig. 2C). However, there is

substantial upwelling only over the time period from May 16 to 20, hence those parcels are the only ones that realize that high phytoplankton production (Fig. 2D). The production in those parcels is observed in the time series samples taken at the D2 mooring from May 19 to 25 (Fig. 10 in Wilkerson et al., 2006), and also observed in the moored instruments (Fig. 1 in Kaplan and Largier, 2006). Note that for the dates shown, the pulse of productivity on May 19–25 was one of the dominant pulses in 2001, but was preceded by the pulse from parcels upwelled on May 10 (seen in Fig. 1 of Kaplan and Largier, 2006).

4. Analysis and results

We are primarily interested in how characteristics of the wind, such as the mean, the variance of the wind speed and the associated time scales of variability; affect biological productivity. For this analysis, we do not examine the effects of the hourly scale time lags between wind speed and water velocity, rather we assume that our approach to calculation of MLD and Ekman transport minimizes their effects on our results. This is reasonable given that observed MLD cross-shelf transports lag wind forcing by 7 h or less (Dever et al., 2006). We are interested in variability in productivity on both synoptic (or upwelling event) and annual time scales. This variability will depend on the relative values of various time scales, which we define here: T_{cs} is the mean cross-shelf transit time, T_P is the time to maximum cumulative phytoplankton in a parcel (defined as the point on Fig. 4 where a line through the origin is tangent to the curve; Botsford et al., 2003), T_Z is the time to maximum cumulative zooplankton in a parcel (defined the same way), and τ_w is the dominant time scale of variability in the wind. We analyze several different cases that illustrate the dependence of productivity on upwelling rate.

4.1. Production per parcel, $F(T)$, held constant

From Eq. (1), if $F[T(t)]$ is constant, shelf productivity, $B(t)$, will trivially be represented by cross-shelf velocity, which in this model is proportional to volume rate of upwelling.

4.1.1. Complete realization of potential new production

Solutions to Eq. (3) indicate that after a particle is upwelled to the surface, conversion of nutrients to phytoplankton and conversion of phytoplankton to zooplankton proceed to a constant level, the maximum potential primary and secondary new production (Fig. 4). The most obvious way that F can be constant is if the mean transport time is long enough for complete realization of potential new production, and the standard deviation of transport time is relatively low. If the transport times for all parcels are long enough that cumulative production is always on the flat part of the curves in Fig. 4 (i.e., $T_{cs} > T_P$, $T_{cs} > T_Z$), productivity will vary with velocity only (Eq. (1)). In this case, the conventional upwelling index (i.e. volume upwelled) will faithfully represent the variability in productivity.

For the parameter values appropriate for the WEST study site, distributions of shelf transit times from our model (Fig. 4) only occasionally allowed for complete realization of maximum potential primary new production, and rarely allowed for complete realization of potential secondary new production (5 and 9.6 days, respectively). Furthermore, box plots of variability from NDBC Buoy 13 winds within specific years (Fig. 5) indicated that this held true for most years. Thus, the upwelling index may not represent the variability in shelf productivity at the WEST location, though it would at other locations with wider shelves and lower wind speeds.

4.1.2. Incomplete realization of potential new production: short and long time scales

For situations with stronger upwelling winds and narrower shelves such that this condition (i.e., T long enough for cumulative shelf production to be on the flat part of the curves in Fig. 4) does not hold, it appears from Eq. (1) that F can still be constant (and productivity will be proportional to upwelling index) if the shelf transit time, T, is constant. To understand how T varies, we differentiate Eq. (7) to obtain,

$$\frac{dT}{dt} = \frac{v(t)}{v(t+T)} - 1. \tag{8}$$

Thus, changes in transit time, T, are determined by values of velocity separated by a time interval equal to the current value of T.

From this we can draw conclusions for several cases. First, if the time scale of the winds is such that the time scales of variability in cross-shelf velocities are much greater than the mean transit time ($\tau_v \gg T_{cs}$), then $v(t)/v(t+T)$ will always be near 1.0, and from Eq. (8), T will vary little. We also can conclude that if the time-scales of variability in the

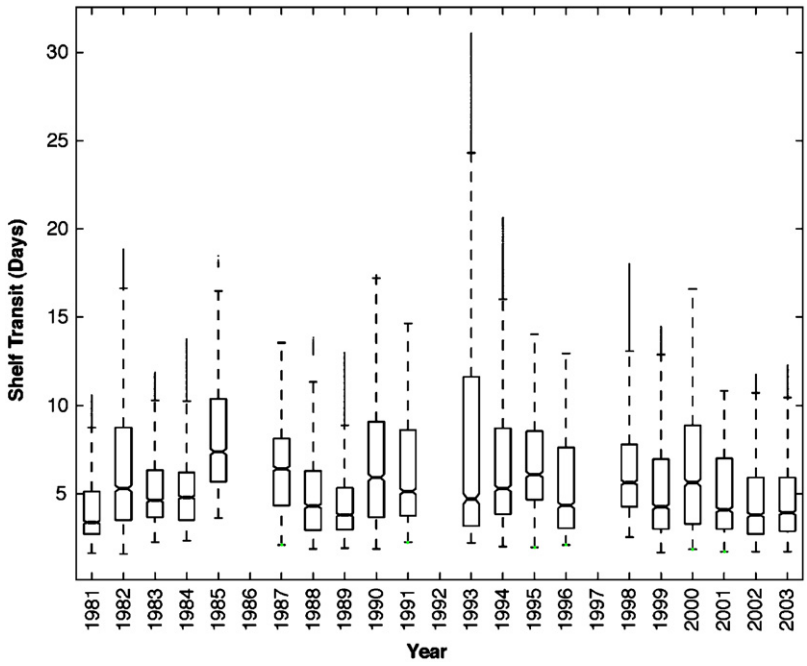

Fig. 5. Box plots of the distributions of shelf transit times computed from NDBC Buoy13 over the 20 years shown in Fig. 3.

cross-shelf velocities are very small with respect to the mean shelf transit time ($\tau_v \ll T_{cs}$), T should again be relatively constant. If time scales of variability in $v(t)$ are small, $v(t)$ and $1/v(t+T)$ will be independent, and the expected value of dT/dt will be

$$E\left[\frac{v(t)}{v(t+T)}\right] - 1 = E[v(t)]E\left[\frac{1}{v(t)}\right] - 1. \quad (9)$$

For high mean velocities, and relatively low variability, these means will be approximately the inverse of each other and dT/dt will be zero. However, if variability in cross shelf velocity is relatively large with respect to the mean velocity, this will not be true. One such case of particular importance here is when variability in velocity can approach zero. From Eq. (8), it is obvious that large changes in cross-shelf transit time would occur if cross-shelf velocities passed through zero. Since relaxation of upwelling winds to near zero is a common occurrence at this location and others, this consideration is important.

For NDBC Buoy 13 winds and the parameter values appropriate for our WEST study area, these conditions of very high and very low time scales of variability with respect to T_{cs} occur only occasionally; the time scales of the cross-shelf velocity through an upwelling season are typically about the same as the mean transit time.

Autocorrelations of winds from Buoy 13 over the past 20 years indicate time scales vary between 3 and 10 days (Fig. 6), values not very different from the mean transit times in Fig. 5. On the other hand, as noted below, there is one period in 2001 in which there are no relaxations, and the cross-shelf velocity varies on a much shorter time scale than the cross-shelf transit time.

4.2. Production per parcel, $F(T)$, not constant

To examine the remaining cases in which $F(T)$ is not necessarily constant, we use time series correlation as an indicator of similarity between the volume upwelled and biological productivity as represented by the model presented here. Relationships between biological variables and upwelling are commonly established on the basis of correlations computed between time series of the conventional upwelling index and time series of biological variables. We assess covariability on two time scales commonly of interest to biologists, the synoptic or event time scale, and the annual time scale.

4.2.1. Effect of common terms

In comparing volume upwelled, which is proportional to cross shelf velocity, $v(t)$, to biological

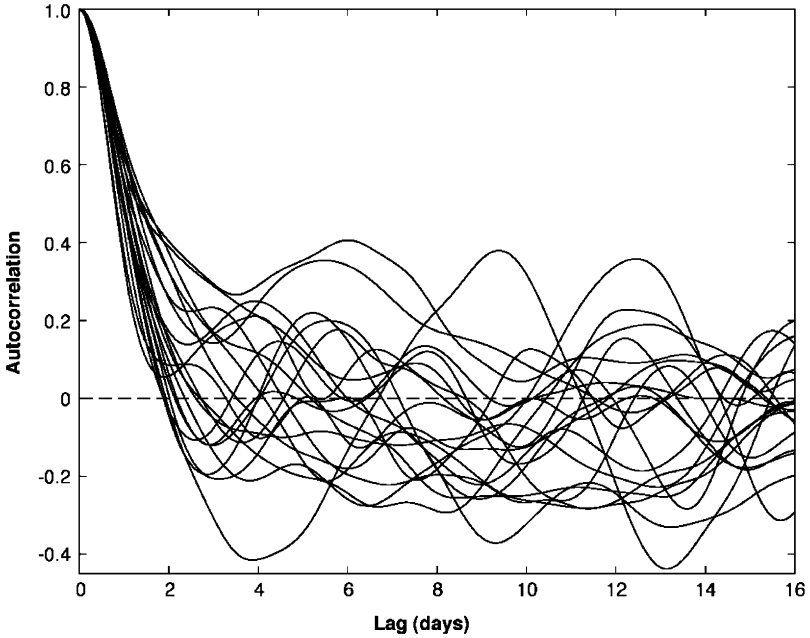

Fig. 6. Autocorrelations of NDBC13 winds in the months of May–July over the years shown in Fig. 4.

production, which is the product of cross shelf velocity and cumulative production (i.e., $v(t)F[T(t)]$), we essentially are computing the correlation between a random series and the product of that random series and another random series, the two of which may or may not be correlated. It is clear that the correlation would be moderately high even if the two series v and F were independent. Moreover, it is also clear that if v goes to zero frequently the correlation should increase. To gain some sense of what to expect from this situation, we examined the correlation between two random series $x(t)$ and $x(t)y(t)$, where $x(t)$ and $y(t)$ are composed of independent Gaussian random variables filtered to have the same time scales as cross-shelf velocities, as we varied the fraction of time that $x(t)$ spends at zero (Fig. 7). Note that as the fraction of time spent at zero by $x(t)$ (and therefore $x(t)y(t)$) increases from 0 to 30%, the correlation increases from a value near 0.6 to greater than 0.9.

Correlations between upwelling and biological production are often assessed on a seasonal or annual time scale. To determine how the computed correlations can be expected to differ at that scale, we computed correlations between the same synthetic data from two series $x(t)$ and $x(t)y(t)$ except that in this instance, we summed each series over a 2-month period before computing the correlations. The results (Fig. 7) indicate a weaker correlation between 0.5 and 0.7, even with a substantial fraction of zeroes in $x(t)$. The question of whether there is a correlation between upwelling rate and production then depends on whether the inverse relationship between $v(t)$ and $F[T(t)]$ will outweigh this moderate positive correlation due to synchronous periods of low values in the two series.

4.3. Expectations from actual wind data

4.3.1. Event time scale

We assessed the similarity between volume upwelled and model biological productivity by computing the correlation between hourly values of volume upwelled and phytoplankton and zooplankton production in the parcel of water upwelled. We chose hourly values to avoid the noise that would be introduced by converting these data to daily averages. We computed the correlations over a running 10-day time periods from April 30 to July 19 in 2001. The 10-day period was chosen to be long enough to produce a reasonable estimate of correlation, while at the same time being short enough to show variability in correlation over different time periods.

The resulting correlations indicate high covariability up to the 10-day period ending on June 13, where they drop to low values, then immediately begin a return to high values (Fig. 8). This behavior

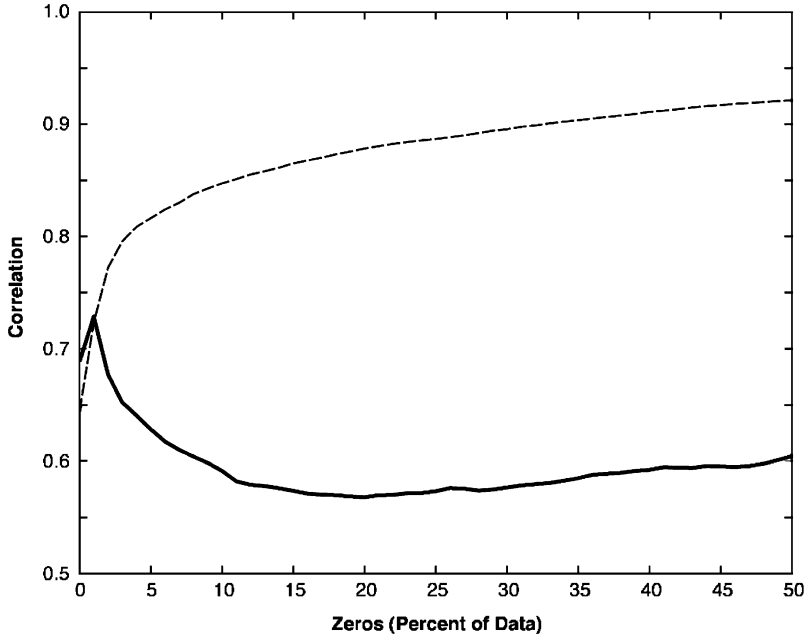

Fig. 7. Correlation between two random time series $x(t)$ and $x(t)y(t)$, where both $x(t)$ and $y(t)$ are independent white hourly series of Gaussian random variables filtered to have roughly the same frequency content as cross-shelf transit times, as the fraction of time spent at zero by $x(t)$ is varied by reducing the mean of the series and setting negative values to zero. The top line (dashed) represents daily correlations, while the bottom line (solid) is for correlations of sums of each series over 90 days, to represent inter-annual covariability in upwelling seasons.

is due to two different mechanisms. In the period from May 2 to June 2 there are frequent excursions of volume upwelled to zero (i.e. relaxations), while during the period from June 3 to 26 there are no zeros, then from June 27 frequent zeros resume to July 19. The fraction of time spent at zero or less by cross-shelf velocity $v(t)$ in the time period from May 2 to June 3 is 0.21. High correlations during this period with frequent zeros are due to the synchronous periods of low values in the velocity and the production time series as indicated by Fig. 7. High correlations during the period without zeros are due to the mechanism described earlier (Section 4.1.2) in which variability in velocity at fast time scales (relative to cross-shelf velocity, T_{cs}) leads to relatively constant T, hence constant F. Note in Fig. 2B that cross-shelf transit time, hence F (Fig. 2C) is relatively constant over the time period June 7–23, even though velocity is fluctuating rapidly (Fig. 2A).

A unique feature of these correlations is the low correlation at June 16. This is caused by the shift between the two mechanisms. The correlation for the period ending near June 10 includes the period of low values in the first few days of June, but after June 12 the effect of those few days declines. The correlation begins to increase again as the end of the period approaches June 17, as the correlation begins to include the period of constant F and the consequent high correlation.

4.3.2. Annual time scale

To compare the inter-annual variability in production of phytoplankton and zooplankton that would be projected by this model, to the conventional volume-based index, we computed the production from May 1 to June 15 for 20 years preceding 2004, then the cross correlation between the volume-based index for that same 45 days and both phytoplankton and zooplankton production (Fig. 9A). To determine the relative amount of inter-annual variability in production that would be expected if advective losses were considered, we also compared the coefficients of variation of each (Fig. 9B). These results were obtained for winds from the NDBC Buoy 13. Data for 1993 were not included because the period of interest in 1993 had an anomalously long 24-day relaxation starting on May 10. This year would have had a disproportionate effect on the inter-annual statistical calculations so it was treated as an outlier. To obtain results of more general applicability, we plotted

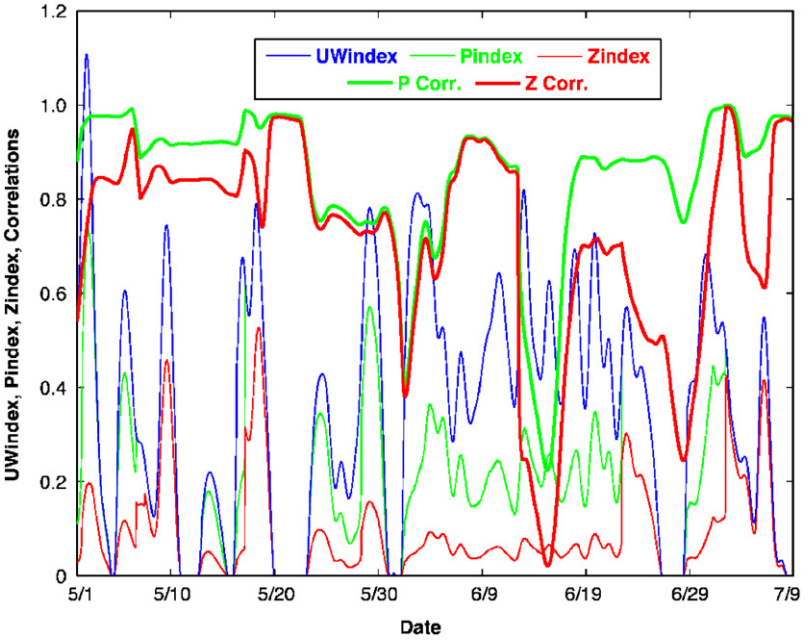

Fig. 8. Running correlation over the previous 10 days, between volume upwelled at time t (UWindex, blue line) and production of phytoplankton (Pindex, green line) and zooplankton (Zindex, redline) from that volume. Correlations are shown as the thick green line and the thick red line for phytoplankton and zooplankton, respectively. Units are the same as in Fig. 1D.

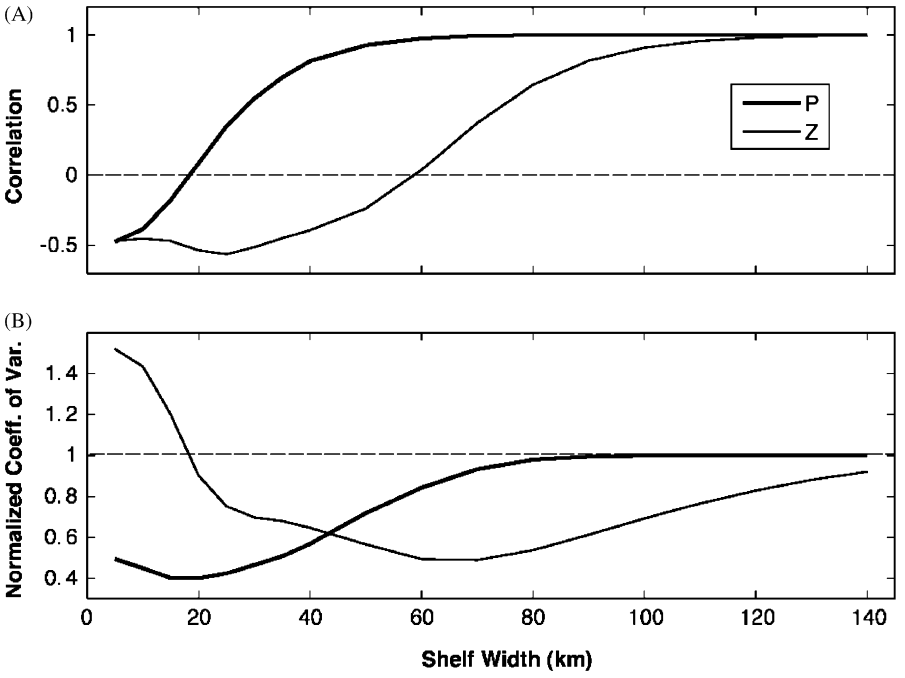

Fig. 9. The correlation between annual values of upwelled volume and annual new production of phytoplankton and consequent zooplankton production (A) and the coefficient of variation of annual new production of phytoplankton and zooplankton normalized by the coefficient of variation of upwelled volume (B). Values were generated from NDBC13 winds and the MLC model described here. Both are plotted against shelf width for generality; the local WEST shelf width is 35 km.

both of these over a range of shelf widths possible in upwelling regions (specific to latitudes 38.2°N or S because of the Coriolis parameter in Eq. (3b)).

Biological production would be highly correlated with upwelling only for shelf widths of 50 km and greater for phytoplankton, and approximately 100 km and greater for zooplankton (Fig. 9A). For narrower widths, correlations decrease and become negative reaching values near −0.5. The amount of variability in annual shelf production due to wind-induced coastal upwelling also would vary with shelf width (as well as latitude and mean winds). As shelf width narrows, the coefficient of variation (CV) of phytoplankton production declines from being the same as the CV of upwelling to 40–60 percent over the range plotted (Fig. 9B). The CV of zooplankton production also declines from being the same as the CV of upwelling as the shelf width declines from high values (not shown), and then increases beginning at a shelf width of about 60 km. However, from Fig. 9A, the increase occurs over values for which the correlation with upwelling is negative.

These differences can be understood by examining them in the context of the dome-shaped response that one would expect from the constant wind case (Botsford et al., 2003) (Fig. 10). In the case with constant wind, as wind speed increases from zero, production increases, up to a point beyond which advective losses off the shelf cause production to decrease. The shelf transit time corresponding to that critical wind speed, i.e. the transit time below which production decreases, is the point on the cumulative production curves in Fig. 4, at which a line through the origin is tangent with the cumulative production curve (Botsford et al., 2003). From Fig. 4, these transport times are 5 and 9.6 days for phytoplankton and zooplankton, respectively. These values correspond to upwelling indices of 4.0 and 1.7, for a shelf width of 35 km, leading to the dome-shaped responses (solid line) in Fig. 10A and D, respectively.

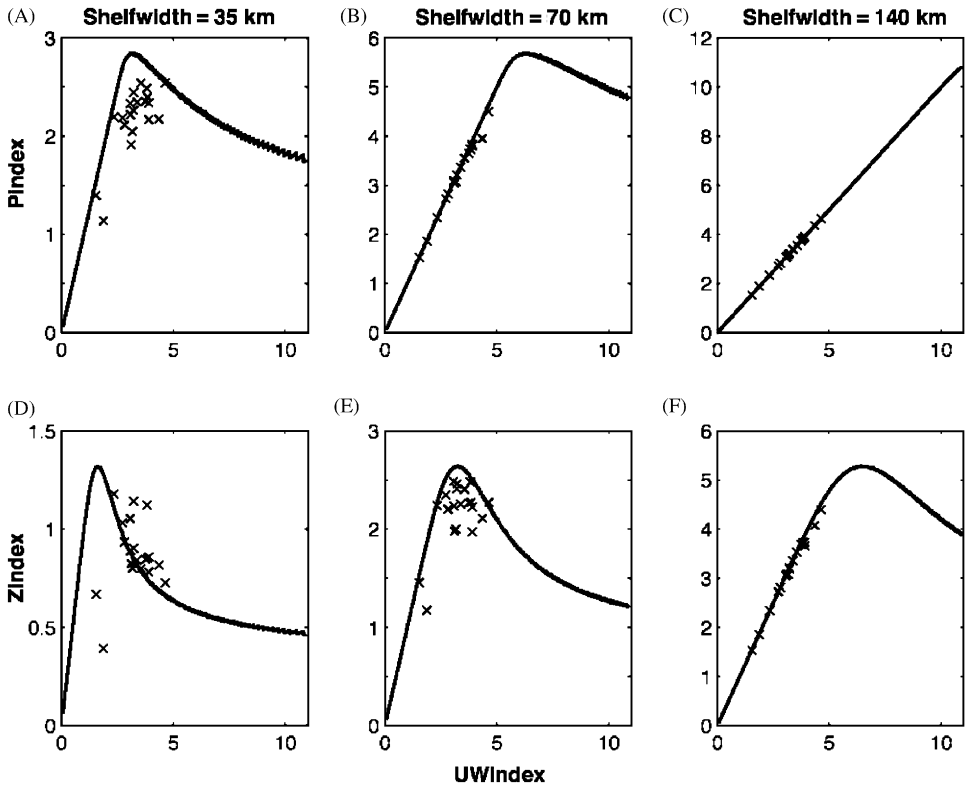

Fig. 10. Annual new production of phytoplankton and zooplankton plotted versus upwelled volume for the 20 years in Fig. 4, for three different shelf widths (*x*'s). Also plotted are the production from the MLC model with constant winds (lines, similar to Botsford et al., 2003) and the annual values of production that would have resulted from the same distribution of wind speeds, but with constant winds through the "lifetime" of the upwelled parcel (circles). Units are the same as in Fig. 1D.

The values of annual phytoplankton production are the same as those for the constant wind case for a shelf width of 140 km, indicating that this width is adequate for complete realization of potential new production (Fig. 10C). As the shelf width becomes narrower (Fig. 10B and A), annual phytoplankton production falls below the values produced under constant winds. Annual zooplankton production for a shelf width of 140 km (Fig. 10F) falls to the left of the peak for the constant wind case and just below the constant wind values. For narrower shelves, values are below the peak (Fig. 10E) and to the right of the peak and greater than the constant wind values (Fig. 10D).

The differences between the responses to constant and variable winds can be understood using Jensen's inequality as a heuristic guide (for another biological example, see Chesson, 1985). According to Jensen's inequality, if the response (productivity) to the input (winds) is either concave up or down (fixed sign of the second derivative of the function) over the range of non-time-varying inputs, then the result of increasing variability while holding the mean constant would be to increase or decrease (respectively) the mean of the response. This occurs because points resulting from varying the independent variable about a point on a curved line will take on values either above or below the tangent at the mean value.

We can explain the differences between values of annual production from constant wind and actual variable winds by considering the distribution of winds, therefore transit times, within years and the consequent cumulative production (Fig. 4), For a wide shelf and short time scale of productivity (Fig. 10C), shelf transit times are always greater than 5 days so that production per parcel is constant (Fig. 4); hence production is proportional to upwelling velocity. As the shelf becomes narrower (Fig. 10B), some transit times within years will be less than 5 days, and production per parcel will be less than the maximum value. Values of upwelling index corresponding to the transit times will range from zero to values above the seasonal means or upwelling index at which each point in Fig. 10B is plotted; hence values of production for those points will be less than the value for constant winds, even though the mean value of upwelling index is in the range of increasing production for constant winds. This means that the points in Fig. 10B can lie below the line corresponding to constant winds, but cannot lie above the increasing part of that line. As shelf width becomes shorter still (Fig. 10A), more transit times will be less than 5 days. However, because the values of transit times in any specific year include values corresponding to values of upwelling index to the left of their mean, the points on Fig. 10A can lie above the descending part of the curve from constant winds. The trend of increasingly shorter times for production relative to the time required for maximal production, with constant winds can be followed by turning to Fig. 10E, where the cloud of points is roughly at the same point relative to the peak. The cloud of points continues to the right in Fig. 10D, but variability in production increases, in part because of an increasing slope reflected in the constant wind line, but also because of the decreasing time over which randomly varying velocity is summed to reach the edge of the shelf.

4.4. Sensitivity to assumptions

To examine the sensitivity of our results to the rate parameter for phytoplankton production (V_m), we computed time series of production per parcel for values of times required for complete uptake (T_P) ranging from 2 to 10 days (Fig. 11). As the time required for complete uptake decreased, the production per particle increased. Over most of this range, temporal patterns were quite similar to each other, with each result being a multiple of the others. However, as the rates approached values of 2 days, the amount of time for which phytoplankton production per upwelled parcel was a maximum dominated the time series, and they were not similar to the others. For the values of rate parameters corresponding to 4 days and greater, it appears that the results obtained here regarding the temporal correlation between upwelling rate and production would hold, based on the similarity in temporal pattern. For shorter uptake times, as the fraction of parcels for which uptake is complete increased to 1.0, the dependence of production on upwelling rate at inter-annual time scales (Fig. 10) would tend to follow the ascending part of the relationship for constant winds, even for a 35 km shelf.

To examine the sensitivity of our results to the use of a simplified surface-mixed layer representation in the MLC, particularly the use of a constant MLD of 17 m for the biological model and a τ-dependent MLD for the physical model, we simulated a fully τ-dependent MLD in which light was explicitly calculated over 30 layers of 1 m depth rather than being averaged. The results of this model are shown

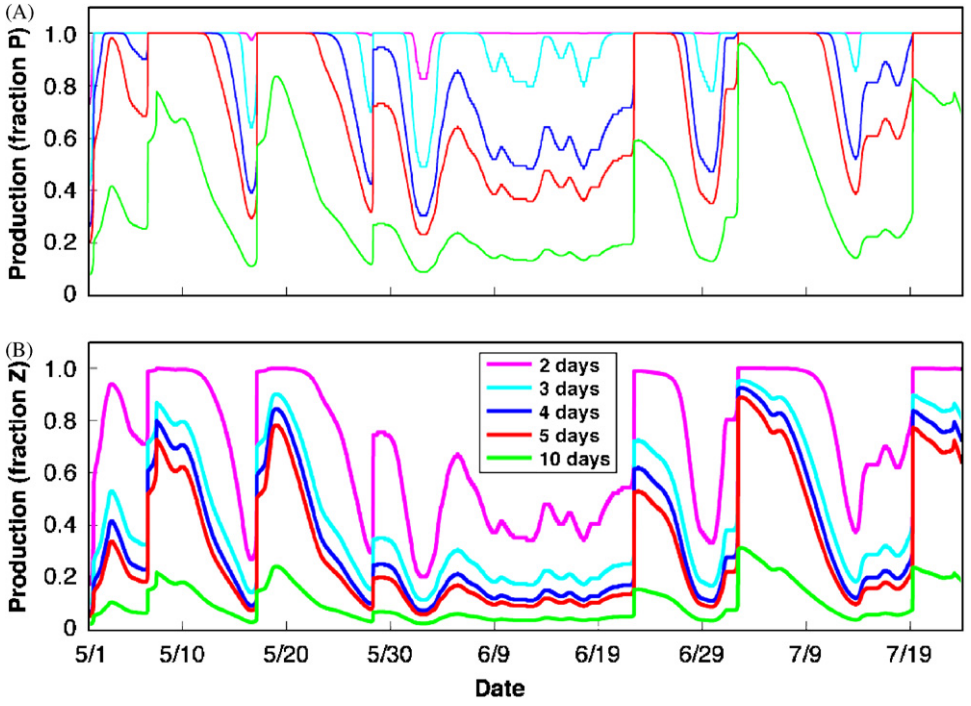

Fig. 11. Sensitivity of results to rate of conversion from nutrients to phytoplankton. Production per parcel for phytoplankton (A) and zooplankton (B) (i.e. comparable to the green and red lines in Fig. 1C).

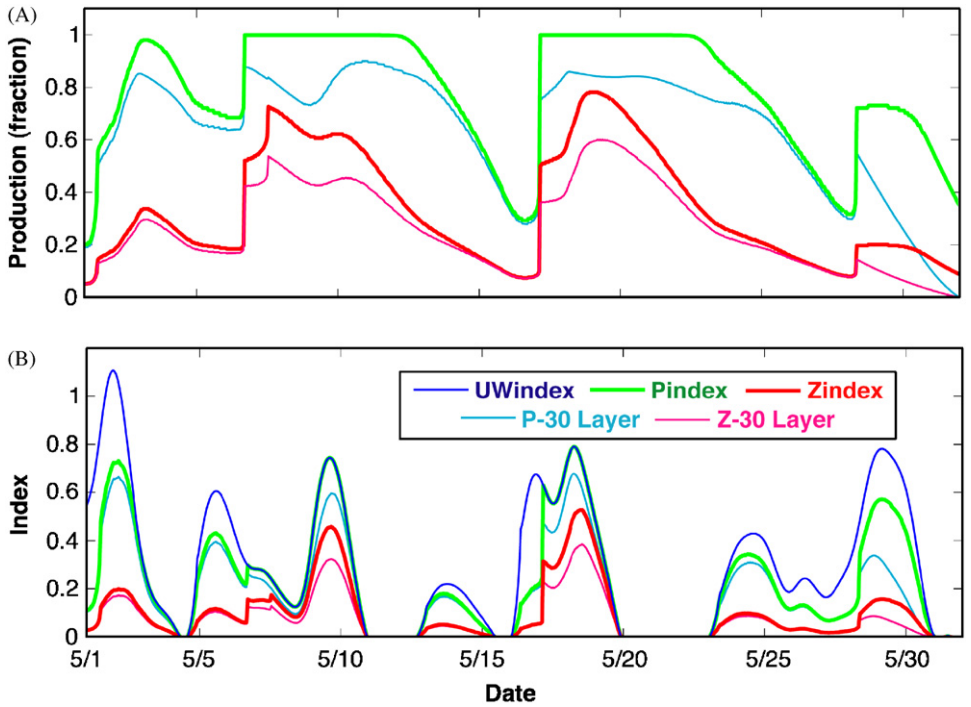

Fig. 12. Sensitivity of model results to relaxation of assumptions about the surface mixed layer. Computation of phytoplankton and zooplankton production under different assumptions regarding the mixed layer depth (A) and their consequences in a comparison to the levels possible with full conversion of nutrients (B). Units of 10B are the same as Fig. 1D.

in Fig. 12 for example year 2001. The alternative approach produced less complete conversion of nutrients to new biological production than our original approach (Fig. 12A); however, this has a minor effect on the volume-weighted production as shown by comparing Figs. 12B–2D. As such, the simplifications we used throughout the analysis represent an upper bound on new biological production. However, the differences are typically so small that they lie within the thickness of the curves in Fig. 11B, giving us confidence that our original assumption did not affect our general results nor their interpretation.

5. Discussion

The dynamics of this simple, idealized MLC model provide a quantitative means for assessing the characteristics of variable wind forcing that motivated the WEST project. This model contains both of the countervailing consequences of winds, (1) upwelling of nutrients, and (2) transport of their biological products away from the local area, allowing us to address long-standing questions regarding how they combine to lead to new production. It provides potential answers to questions such as what is the optimal pattern of strong and weak (or reversed) upwelling winds, and what is the impact of upwelling relaxations on primary productivity? Moreover, it extends our intuition and ability to quantify beyond the concepts of the ideal periods of optimal strong and weak pulses, to the consequences of all forms of variability in upwelling winds. It does this by making explicit assumptions about the spatial characteristics of the process.

The key assumption of this model is spatial limitation of the advective physical/biological process, a necessary element of such a model. Without this spatial limitation there would be fewer questions regarding the effect on production of the temporal pattern in variable upwelling winds. Periods of relaxation would have no special value since there would be no time limit on conversion of nutrients to phytoplankton and higher trophic levels as surface waters were transported downstream. The highest wind possible would be optimal, and production would be correlated with upwelling rate.

In the two-dimensional MLC model considered here and elsewhere (e.g., Mann, 2000), the mechanism for advective loss is the cross-shelf Ekman transport. Biological products transported across the shelf break by the Ekman transport are lost to further trophic development (Botsford et al., 2003). However, the cross-shelf Ekman transport also accelerates an equatorward along-shelf transport.

A detailed examination of possible along-shelf advective loss mechanisms is beyond the scope of this study. However, we can gain some insight as to the relative magnitude of cross-shelf and along-shelf transport by considering a simple two-dimensional model of coastal upwelling. This model was developed by Janowitz and Pietrafesa (1980) and applied with some success by Dever (1997) to the northern California shelf about 60 km north of the WEST region. The model is consistent with the MLC in that there is a wind-forced offshore Ekman transport confined to a distinct surface boundary layer.

In this model, the magnitude of the steady state along-shelf velocity relative to the offshore velocity (Eq. (2a)) depends on the bottom friction. For reasonable values of bottom friction, the steady state value along-shelf velocity is about 6 times the offshore velocity (assuming a MLD of 17 m). Hence during the same time a water parcel travels 35 km to the shelf break, it would travel 210 km in the along-shelf direction if the steady state velocity were achieved. If capes or other large changes in bathymetry exist within this distance (as in the WEST region), then clearly along-shelf advection is a major source of advective loss from the shelf.

The steady state is an upper bound on the magnitude on the along-shelf velocity generated by this model. The time to reach steady state is a function of both the bottom friction and the total water depth. As bottom friction increases, the time to reach steady state decreases. Conversely, as depth increases, the time to reach steady state increases. At typical mid-shelf depths (100 m), the time scale is about 4 days. For wind forcing events shorter than this time, the along-shelf velocity will not be 6 times the cross-shelf velocity, but something closer to twice the cross-shelf velocity (again assuming a MLD of 17 m). This is significantly slower than the steady state along-shelf velocity, and it is interesting to note that similar time scales likely exist for the cross-shelf transit time and the time required for downstream advection to a cape (Pt. Reyes) in the WEST region.

The observations support both cross-shelf and along-shelf advection as likely mechanisms for advective losses from the region. Significant along-shelf transport is observed during WEST where the dominant surface flows are north to south, at an oblique angle to the coastline. HF radar measurements indicate only some surface parcels flow off

the shelfbreak in this region, with the remainder transported to the south (Kaplan and Largier, 2006). Production could be lost to local higher trophic levels downstream at capes where along-shelf transport can leave the coast in upwelling filaments (e.g., Strub et al., 1991; referred to in Ware and Thomson, 2005) or where along-shelf upwelling jets are subducted beneath less dense coastal waters (Collins et al., 2003). Thus downstream along-shelf transport constitutes an important alternative advective loss mechanism.

Our model results presented depend on accurate representation of the effects of wind on the MLD. WEST observations indicate calculation of the MLD from Eq. (3) is adequate for our purposes. Dever et al. (2006), estimate surface boundary layer depths for the WEST region and calculate Ekman transport (relative to the interior flow). They find surface MLDs ranging from 0 (during wind relaxation events) to 40 m or more (during strong upwelling events). The MLD used here is qualitatively consistent with their results. Dever et al. (2006) also calculate observed surface boundary layer transports and find that the observed offshore surface boundary layer transport is well correlated with, and similar in magnitude to, the Ekman transport estimated from wind stress. This finding is well supported by historical results and is common to several coastal upwelling regions (Lentz, 1992).

Our understanding of the effects of time-varying winds on shelf production can be summarized as the combination of two effects: (1) the inverse effect of losses with high winds and (2) the effect of synchronous periods of low values in the time series of upwelling rate and production. These combine and sometimes work at cross-purposes for different levels of average wind and different time scales of interest.

The inverse effect of losses with high winds can be seen in the dome-shaped relationship that resulted for new production only in our earlier investigation of the effects of constant winds (i.e. the lines in Fig. 10). The shape of that relationship is determined by the spatial limitation, which in conjunction with wind speed, sets the dominant physical time scale, here referred to as the cross-shelf transit time (T_{cs}). The dominant physical time scale in comparison with the dominant biological time scales, the time to complete nutrient uptake by phytoplankton (T_P), and the time to maximal zooplanton population development (T_Z) determine the dynamic behavior of production in response to winds. When the dominant biological time scale exceeds the dominant physical time scale, increasing wind strength shifts from having a positive effect to a negative effect in a way that is transparent for constant winds.

The effect of synchronous periods of low values in the wind and the production series (due to wind relaxations) arises when temporal variability in the wind is introduced. It has two important characteristics: (1) it has a positive effect on the correlation between upwelling rate and production, in spite of the fact that relaxation (low wind) represents an inverse effect on production (high production), and (2) it depends on the time scale of observation, being stronger at the synoptic (event) scale, but still having an effect at the inter-annual scale. The latter characteristic occurs because inter-annual variability involves averaging upwelling rate and production over a season, thus reducing the presence of the shorter time scale.

In addition to these major effects, we also saw that when temporal variability is added, wind variability on time scales (τ_w) either much shorter than or much longer than the dominant physical time scale, T_{cs} can lead to a positive correlation between upwelling rate and production (Section 4.1.2).

The scientific implications of these results depend on the time scale of interest to investigators. On synoptic (event) time scales, prediction of production from winds would be of interest to investigators of event scale effects of productivity on filter-feeding invertebrates in the inter-tidal zone. Their investigations address issues such as the trophic organization of intertidal communities (Menge, 2000) and the geographic variability in abundance and growth rate that could determine species distribution and abundance. They compare growth to synoptic scale variability in upwelling (e.g., Sanford and Menge, 2001) and compare community interactions among areas of the California Current that are differentiated on the basis of the time scales of variability in their upwelling winds (Menge et al., 2004). Our results on synoptic time scales are also relevant to feeding and growth of nearshore rockfish, whose feeding behavior is influenced synoptic scale variability in upwelling (Hobson and Chess, 1988).

Strictly speaking our MLC model would not apply shoreward of the depths over which surface Ekman transport divergence (i.e. upwelling) occurred. For the spatially uniform wind forcing consistent with our model, Ekman transport

divergence occurs in depths shallow enough such that there is a direct transfer of the turbulent momentum flux from the surface to the bottom boundary layer. The spatial extent of this region, often called the inner shelf, depends strongly on the interior stratification. The exact spatial extent of the inner shelf is not well known. When stratification exists, the inner shelf can be as shallow as 15–30 m depth (e.g., Lentz, 2001; Kirincich et al., 2005). For the WEST observations, available evidence (Dever et al., 2006) indicates that the 40-m mooring is usually outside the inner shelf for spring 2001. That is, the inner shelf boundary is somewhere between 40 m and the coast, a distance of 1.5 km.

In spite of the fact that the inter-tidal areas are shoreward of these depths, the clear examples of observed effects of synoptic scale variability on inter- and sub-tidal ecology mentioned above indicates the variation in productivity described in our model does affect these areas. Also, since the area of interest for intertidal studies is the near shore, one would expect mechanisms involving losses due to advection out of the area of interest to be particularly relevant. Our results indicate that, in spite of a negative relationship between productivity per parcel upwelled and wind stress, there is likely to be a strong correlation between volume upwelled and productivity. The basis of that correlation is the presence of synchronous periods of low values in volume upwelled and productivity (volume upwelled times productivity per unit volume).

Taken at face value, this suggests that the standard upwelling index remains a useful indicator of productivity, and it can continue to be used to detect the presence and absence of such a relationship. However, this result also indicates that there could be a negative effect of wind on productivity present, yet it would be occluded by the positive effect of the synchronous periods of low values in wind and production. This latter consideration suggests that attempting to detect both effects through use of a model such as the MLC would lead to a more comprehensive description with greater fidelity and usefulness. For example, finding a positive correlation between upwelling and production could lead to the conclusion that there was not an inverse effect of strong winds on productivity, even when it was present.

Turning to the annual time scale where wind effects are commonly summed or averaged over the upwelling period of several months, then compared with annual productivity, the effect of the synchronous periods of low values on signal detection is reduced. For example, the correlation between $x(t)$ and $x(t)y(t)$, where $x(t)$ and $y(t)$ were independent, was near 0.9 for the synoptic time scale, but for the annual time scale dropped to near 0.5 (Fig. 7). In spite of the fact that the effect of synchronous periods of low values on the correlation between upwelling rate and production is real, in attempting to detect the relationship between upwelling winds and production that one would see with constant winds, it introduces a bias in correlation in the direction of a positive relationship. This effect is evident, for example, in the lack of symmetry in Fig. 9A. For broad shelves, when the productivity has a positive dependence on upwelled volume (Fig. 10C), a correlation of 1.0 is possible, however, for narrow shelves, where productivity has a negative dependence on upwelled volume (Fig. 10D), the maximum (negative) correlation is -0.5 (Fig. 9A). Thus, results at the annual scale also suggest a model that includes both the positive and negative aspects of the production process be used to investigate the mechanism(s) by which upwelling and production are related. Another possible alternative, that we adjust for the positive bias that appears to be 0.5 both for artificially generated series (Fig. 7) and for real wind series (Fig. 9A), would be risky since the magnitude of the bias depends on the details of the distribution of wind strengths and the length of the period over which winds are summed or averages. Longer periods would lead to less bias, but it would be difficult to predict the bias on the basis of a single realization of the process.

The use of an MLC model in detection and prediction of the effects of wind variability on biological production apparently would improve those efforts, yet would not place a great additional burden on them. As seen in Eq. (1) it requires only adding an expression of the potential productivity per parcel. The upwelling velocity can be taken from existing calculations of the upwelling index or computed directly from buoy winds, as was done here. Calculation of potential productivity per parcel for new phytoplankton production would not require the full biological model used here, but rather only a means for constructing a cumulative phytoplankton production curve such as that in Fig. 4. The most important aspect of that curve is that it have the correct time scale. Based on observations in a number of areas that time scale is in the range of 3–7 days (Dugdale et al., 2006).

The next step, choosing a spatial scale, is somewhat speculative, as it requires settling on a physical mechanism. The goal would be to characterize the dominant, upwelling-driven flow in the region of interest by choice of the spatial dimension of the model. Because of the uncertainty in the appropriate physical spatial scale and the biological temporal scale, another possibility is to include a general dome-shaped relationship, and fit it to the statistical characteristics of the data by appropriate choice of parameter values.

The lack of a linear increase in production with upwelling velocity as described here may be in part responsible for the lack of consistent relationships between annual upwelling indices and production at higher trophic levels. In the California Current, correlations between Bakun's upwelling index and biological indicators are sometimes found (Botsford and Wickham, 1975; Nickelson, 1986; Botsford and Lawrence, 2002), but just as often are not found. Notably, Nickelson's (1986) correlation between upwelling index and coho salmon became negative and statistically insignificant after the decadal scale shift in ocean conditions in the mid-1970s (Pearcy, 1997). Interpretation of the role of upwelling in detected biological responses is clouded by the fact that the upwelling index (which is computed from atmospheric pressure observations) is highly correlated with other hydrographic indicators that vary with biological production in the CCS (i.e. sea level and temperature) (Botsford and Lawrence, 2002). There is also a long-standing question as to whether wind-induced coastal upwelling is the source of nutrients in this system (Reid, 1962). Alongshore advection from the north was proposed as an alternative based on a lack of correlation between zooplankton and upwelling (Chelton et al., 1982). However, Collins et al. (2003) recently reported direct observations of wind-driven upwelling as the source. Other mechanisms, at least on longer, decadal time scales include the depth of the mixed layer (McGowan et al., 2003). Our results here (i.e. Fig. 10D and E) indicate that even if wind-induced coastal upwelling were driving biological production, there could still be very little annual variability in new production, and that the consequent zooplankton production could be poorly or negatively correlated.

Several observations are consistent with the predicted consequences of the MLC mechanism. A dome-shaped relationship between upwelling winds and meroplankton settlement was described in our earlier analysis of the response of the MLC to constant winds (Botsford et al., 2003). Another local example is the comparison of growth rates of juvenile salmon between years of strong and weak upwelling. Growth rates of Chinook salmon in the Gulf of the Farallones in 1998 and 1999 unexpectedly showed little difference in growth (Botsford, 2002; MacFarlane et al., 2002).

From a global, more spatial perspective, the range of cross-shelf velocities and shelf widths in the four major coastal upwelling regions (Carr and Kearns, 2003) indicate the mechanism studied here could affect expectations regarding productivity. From satellite-derived chlorophyll estimates, Thomas et al. (2003) found that the latitudes of maximum chlorophyll *a* were generally the latitudes of greatest upwelling. From their examination of a number of hydrographic variables, Carr and Kearns (2003) found that spatial and temporal variability was due to the effect of large-scale circulation on source waters, sometimes in conjunction with local wind forcing. Analyses such as these could benefit by considering the potential for advective losses off continental shelves, using calculations such as the MLC model. Indications that the timescales of phytoplankton development are similar between systems (see Wilkerson et al., 2006; Dugdale et al., 2006) imply that the differences between systems may depend on differences in shelf widths, mean winds, the time scale of wind variability and the frequency of relaxations.

The potential global implications of the results obtained here can be understood in terms of the relationships between time scales by defining a characteristic velocity for a location as the ratio of the shelf width (W) to the time scale of biological production (T_P or T_Z), then plotting production from constant winds and variable winds with velocity normalized by that characteristic velocity (Fig. 13). This essentially allows all of the plots in Fig. 10 to be approximated in a single plot. For weak wind and a low relative velocity, the ascending limb of the dome-shaped relationship is followed closely, but as we depart from those conditions, production from variable winds is initially less than that predicted from constant winds, then at some point crosses the descending limb of the constant wind relationship and remains greater than the constant wind relationship, declining more gradually. A critical aspect of this general view is that the locations of the ellipsoids representing variability depend critically on the fact that as we increase the

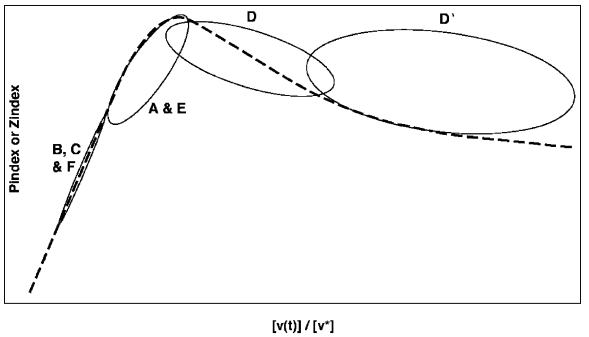

Fig. 13. A schematic view of how productivity varies with a generalized velocity, normalized by dividing by a characteristic velocity associated with the location. The characteristic velocity, v^*, is the shelf width divided by the time scale of biological production.

average normalized velocity, the distribution of winds still contains zeroes (i.e. relaxations).

The MLC model runs presented here compares closely to observations, both in terms of biological and physical processes and the consequences for the dependence of productivity on wind speed and pattern. The biological parameters were chosen to represent typical patterns of new production both in WEST and in other upwelling systems. The time to complete nutrient uptake by phytoplankton in the MLC is about 5 days (Fig. 4), which compares favorably with the duration of 6 days Fig. 11C in Wilkerson et al. (2006) and is within the generally regarded range of 3–7 days (Wilkerson et al., 2006). Sensitivity runs varying drawdown time (Fig. 11) indicate that the results obtained here regarding correlation with upwelling volume on various time scales should hold for all but the fastest times (2 days). The dominant flows in WEST as seen in the HF radar and other data, involve upwelling and transport of water offshore and out of the local area with a spatial scale near 35 km. The time scales of transport off the shelf and out of the local area range from 2 to 6 days, and vary with the wind (Figs. 15 and 16 in Kaplan and Largier, 2006). Additional, more direct comparisons are planned.

Other models and observations show losses off the shelf. A non-spatial version of the model of Fasham et al. (1990) parameterized for upwelling near Monterey, 200 km to the south of the WEST site, produced the result that slightly greater than half of the primary production was exported, and that result compared favorably with field values (Olivieri and Chavez, 2000). From Fig. 10A for the 35-km shelf, projecting the linear part of the phytoplankton production curve to higher upwelling values so that the offshore losses are ignored shows that the values of production we obtain here are just greater than half of the projected linear values at the mean upwelling value. From hydrographic observations near Monterey Bay in central California, Collins et al. (2003) identified subduction beneath the coastal jet as a potential mechanism for offshore loss at that location.

We have used an idealized model here raising the question of the effects of factors not directly accounted for. We explicitly evaluated the effects of leaving the wind-driven variability in the MLD out of the production calculation. It affects the scale of the production, but not the temporal pattern, which is the focus here. A similar comment can be made regarding sinking; to a first approximation, the influence of sinking on rates of new production are not likely to change with the time scale of forcing. We have not specifically addressed the consequences of the shift-up phenomenon (Zimmerman et al., 1987), but it is represented to some degree our examination of the range of development rates. Another important effect not accounted for in our model is the tendency of diel vertical migration of some zooplankton to lead to their greater retention on than shelf than the passive particles depicted here (Batchelder et al., 2002). Lastly, the MLC model is not well suited for easy incorporation of the recent WEST results involving upwelling due to wind stress curl (Dorman et al., 2005), but to the degree that the curl is correlated with the magnitude of wind stress (Dorman et al., 2005), the results here would apply.

More complex models could be formulated to include these effects, but that would be at the expense of run times and ease of analysis. Three-dimensional circulation models for the WEST location have been developed (Gan and Allen, 2002a, b; Kuebel Cervantes and Allen, 2005), and the latter includes Lagrangian tracers, a capability that would be useful in the context of the topic here. A two-dimensional "slice" model (Spitz et al., 2003) and a model that advects NPZ models along a characteristic line (Newberger et al., 2003) have been used to assess the cross-shelf spatial distribution of biological material. An approach that compared the mechanisms and effects described here among models of varying complexity is a reasonable way to pursue further investigation of the consequences identified in this simple, idealized model. Such an approach could also explore some

of the mechanisms not accounted for here, such as diel vertical migration of zooplankton.

6. Conclusions

Adding temporal variability in winds to an MLC model that appears to reflect the relationship between observations of chlorophyll, wind, and surface transport in the WEST program has revealed that high winds can have an inverse effect on new production. The common practice of computing correlations between time series of upwelled volume and biological variables is attempting to detect a biologically meaningful effect of upwelling, but the resulting covariability is due to two mechanisms, (1) the effect of wind on production, and (2) the effect of synchronous periods of low values. The former can tend to produce more negative correlations, and the latter more positive correlations. The effects of time-varying winds and upwelling on biological production are in this sense very different from conclusions we might reach viewing the process as merely a noisy version of constant upwelling. Accounting for the possibility of an inverse relationship using a model similar to the MLC may be useful in increasing our understanding of variability in new production on both synoptic (event) and inter-annual time scales.

Acknowledgments

Funding was provided by the NSF Coastal Ocean Processes (CoOP) program (LWB, CAL and AH funded by OCE-9910897) (EPD and JLL funded by OCE-9907884). This work benefited greatly from discussions with our WEST colleagues, especially Dick Dugdale, Frances Wilkerson, David Kaplan, and Raphe Kudela. We also thank the anonymous reviewers for their comments.

References

Bannister, T.T., 1974. A general theory of steady state phytoplankton growth in a nutrient saturated mixed layer. Limnology and Oceanography 19, 13–30.

Bakun, A., 1973. Coastal upwelling indices, west coast of North America, 1946–1971. NOAA Technical report, NMFS SSRF-671, 103pp.

Batchelder, H.P., Edwards, C.A., Powell, T.M., 2002. Individual-based models of copepod populations I: coastal upwelling regions: implications of physiologically and environmentally influenced diel vertical migration on demographic success and nearshore retention. Progress in Oceanography 53, 307–333.

Beardsley, R.C., Limeburner, R., Rosenfeld, L.K., 1985. Introduction to the CODE-2 moored array and large-scale data report. In: Limeburner, R. (Ed.), CODE-2: Moored Array and Large-scale Data Report. WHOI Technical report, WHOI-85-35, 234pp.

Botsford, L.W., 2002. Ocean influences on Central Valley Salmon: the rest of the story. IEP Newsletter 15, 47–52.

Botsford, L.W., Wickham, D.E., 1975. Correlation of upwelling index and Dungeness crab catch. US Fishery Bulletin 73 (4), 901–907.

Botsford, L.W., Lawrence, C.A., 2002. Patterns of co-variability among California current Chinook salmon, Coho salmon, Dungeness crab, and physical oceanographic conditions. Progress in Oceanography 53, 283–305.

Botsford, L.W., Lawrence, C.A., Dever, E.P., Hastings, A., Largier, J., 2003. Wind strength and biological productivity in upwelling systems: an idealized study. Fisheries Oceanography 12, 245–259.

Carr, M.-E., 1998. A numerical study of the effect of periodic nutrient supply on pathways of carbon in a coastal upwelling regime. Journal of Plankton Research 20, 491–516.

Carr, M.-E., Kearns, E.J., 2003. Production regimes in four Eastern boundary current systems. Deep-Sea Research II 50, 3199–3221.

Chelton, D.B., Bernal, P.A., McGowan, J.A., 1982. Large-scale interannual physical and biological interaction in the California Current. Journal of Marine Research 40, 1095–1125.

Chesson, P.L., 1985. Coexistence of competitors in spatially and temporally varying environments: a look at the combined effects of different sorts of variability. Theoretical Population Biology 28, 263–287.

Collins, C.A., Pennington, J.T., Castro, C.G., Rago, T.A., Chavez, F.P., 2003. The California current system off monterey, California: physical and biological coupling. Deep-Sea Research II 50, 2389–2404.

Cury, P., Roy, C., 1989. Optimal environmental window and pelagic fish recruitment success in upwelling areas. Canadian Journal of Fisheries and Aquatic Sciences 46, 670–680.

Cushing, D.H., 1971. Upwelling and the production of fish. Advances in Marine Biology 9, 255–334.

Dever, E.P., 1997. Wind-forced cross-shelf circulation on the northern California shelf. Journal of Physical Oceanography 27, 1566–1580.

Dever, E.P., Dorman, C.E., Largier, J.L., 2006. Surface boundary layer variability during spring and summer upwelling. Deep-Sea Research II, accepted for publication.

Dorman, C.E., Dever, E.P., Largier, J., Koracin, D., 2005. Buoy measured wind, wind stress and wind stress curl over the shelf off Bodega Bay, California. Deep-Sea Research II.

Dugdale, R.C., Wilkerson, F.P., Marchi, A., Hogue, V.E., 2006. Nutrient Controls on New Production in the Bodega Bay, California, coastal upwelling plume. Deep-Sea Research II, submitted for publication.

Edwards, C.A., Powell, T.A., Batchelder, H.P., 2000. The stability of an NPZ model subject to realistic levels of vertical mixing. Journal of Marine Research 58, 37–60.

Fasham, M.J.R., Ducklow, H.W., McKelvie, S.M., 1990. A nitrogen-based model of the plankton dynamics in the ocean mixed layer. Journal of Marine Research 48, 591–639.

Franks, P.J.S., Walstad, L.J., 1997. Phytoplankton patches at fronts: a model of formation and response to wind events. Journal of Marine Research 55, 1–29.

Gan, J., Allen, J.S., 2002a. A modeling study of shelf circulation off northern California in the region of the Coastal Ocean dynamics experiment: response to relaxation of upwelling winds. Journal of Geophysical Research 107, 3123.

Gan, J., Allen, J.S., 2002b. A modeling study of shelf circulation off northern California in the region of the Coastal Ocean dynamics experiment 2: simulation and comparisons with observations. Journal of Geophysical Research 107, 3184.

Hobson, E.S., Chess, J.R., 1988. Trophic relations of the blue rockfish, Sebastes mytinus, in a coastal upwelling system off northern California. Fishery Bulletin of the United States of America 86, 715–743.

Hofmann, E.E., Ambler, J.W., 1988. Plankton dynamics on the outer southeastern U.S. continental shelf. Part II: a time-dependent biological model. Journal of Marine Research 46, 883–917.

Janowitz, G.S., Pietrafesa, L.J., 1980. A model and observations of time-dependent upwelling over the mid-shelf and slope. Journal of Physical Oceanography 10, 1574–1583.

Kaplan, D.M., Largier, J.L., 2006. HF-radar-derived origin and destination of surface waters flowing past Bodega Bay, California. Deep-Sea Research II, submitted for publication.

Kirincich, A.R., Barth, J.A., Grantham, B.A., Menge, B.A., Lubchenco, J., 2005. Wind-driven inner-shelf circulation off central Oregon during the summer. Journal of Geophysical Research 110, C10S03.

Kudela, R.M., Dugdale, R.C., 2000. Nutrient regulation of phytoplankton productivity in Monterey Bay, California. Deep-Sea Research II 47, 1023–1053.

Kuebel Cervantes, B.T., Allen, J.S., 2005. Numerical model simulations of continental shelf flows off northern California. Deep-Sea Research II, accepted for publication.

Lasker, R.L., 1975. Field criteria for survival of anchovy larvae: the relation between inshore chlorophyll maximum layers and successful first feeding. Fishery Bulletin of the United States of America 73, 453–462.

Leet, W.S., Dewees, C.M., Klingbeil, R., Larson, E.J., 2001. California's Living Marine Resources: A Status Report, 592pp.

Lentz, S.J., 1992. The surface boundary layer in coastal upwelling regions. Journal of Physical Oceanography 22, 1517–1539.

Lentz, S.J., 2001. The influence of stratification on the wind-driven cross-shelf circulation over the North Carolina shelf. Journal of Physical Oceanography 31, 2749–2760.

MacFarlane R.B., Ralston, S., Royer, C., Norton, E.C., 2002. Influences of the 1997–1998 El Niño and 1999 La Nina on juvenile Chinook salmon in the Gulf of the Farallones. PICES MODEL/REX report 20, pp. 25–29.

Mann, K.H., 2000. Ecology of Coastal Waters, with Implications for Management, second ed. Blackwell Science, Boston, 406pp.

McGowan, J.A., Bograd, S.J., Lynnh, R.J., Miller, A.J., 2003. The biological response to the 1977 regime shift in the California Current. Deep-Sea Research II 50, 2567–2582.

Menge, B.A., 2000. Top-down and bottom-up community regulation in marine rocky intertidal habitats. Journal of Experimental Marine Biology and Ecology 250, 257–289.

Menge, B.A., Blanchette, C., Raimondi, P., Freidenburg, T., Gaines, S., Lubchenco, J., Lohse, D., Hudson, G., Foley, M., Pamplin, J., 2004. Species interaction strength: testing model predictions along an upwelling gradient. Ecological Monographs 74, 663–684.

Moloney, C.L., Field, J.G., 1991. The size-based dynamics of plankton food webs 1. A simulation model of carbon and nitrogen flows. Journal of Plankton Research 13, 1003–1038.

Newberger, P.A., Allen, J.S., Spitz, Y.H., 2003. Analysis and comparison of three ecosystem models. Journal of Geophysical Research 0, 108.

Nickelson, T.E., 1986. Influences of upwelling, ocean temperature and smolt abundance on marine survival of coho salmon (*Oncorhynchus kisutch*) in Oregon production area. Canadian Journal of Fisheries and Aquatic Sciences 43, 527–535.

Olivieri, R.A., Chavez, F.P., 2000. A model of plankton dynamics for the coastal upwelling system of Monterey Bay, California. Deep-Sea Research II 47, 1077–1106.

Parrish, R.H., Bakun, A., Husby, D.M., Nelson, C.S., 1983. Comparative climatology of selected environmental processes in relation to eastern boundary current pelagic fish reproduction. In: Sharp, G.D., Csirke, J. (Eds.), Proceedings of the Expert Consultation to Examine Changes in Abunndance and Species Composition of Neritic Fish Resources, San Jose, Costa Rica, April 1983, vol. 291. F.A.O. Fish. Rep., pp. 731–777.

Pearcy, W.G., 1997. Salmon production in changing ocean domains. In: Stouder, D.J., Bisson, P.A., Naiman, R.J. (Eds.), Pacific Salmon and Their Ecosystems: Status and Future Options, pp. 331–352.

Peña, M.A., 1994. New production in the tropical Pacific region. Ph.D. thesis, Dalhousie University.

Peterson, W.T., 1973. Upwelling indices and annual catches of Dungeness crab, Cancer magister, along the west coast of the United States. Fishery Bulletin of the United States of America 71, 902–910.

Pollard, R., Rhines, P.B., Thompson, R.O.R.Y., 1973. The deepening of the wind-mixed layer. Geophysical Fluid Dynamics 3, 381–404.

Reid, J.L., 1962. On the circulation, phosphate-phosphorus content and zooplankton volume in the upper part of the Pacific Ocean. Limnology and Oceanography 7, 287–306.

Ryther, J.H., 1969. Photosynthesis and fish production in the sea. Science 166, 72–80.

Sanford, E., Menge, B.A., 2001. Spatial and temporal variation in barnacle growth in a coastal upwelling system. Marine Ecology-Progress Series 209, 143–157.

Send, U., Beardsley, R.C., Winant, C.D., 1987. Relaxation from upwelling in the coastal ocean dynamics experiment. Journal of Geophysical Research 92, 1683–1698.

Spitz, Y.H., Newberger, P.A., Allen, J.S., 2003. Ecosystem response to upwelling off the Oregon coast: behavior of three nitrogen-based models. Journal of Geophysical Research, 108.

Strub, P.T., Kosro, P.M., Huyer, A., 1991. The nature of cold filaments in the California current system. Journal of Geophysical Research-Oceans 96 (C8), 14743–14768.

Thomas, A., Strub, P.T., Carr, M.E., Weatherbee, R., 2003. Comparisons of chlorophyll variability between the four major global eastern boundary currents. International Journal of Remote Sensing 25, 1443–1447.

Trenbreth, K.E., Large, W.G., Olson, J.G., 1990. The mean annual cycle in global ocean wind stress. Journal of Physical Oceanography 20, 1742–1760.

Walsh, J.J., 1975. A spatial simulation model of the Pery upwelling ecosystem. Deep-Sea Research 22, 201–236.

Walsh, J.J., Dugdale, R.C., 1971. A simulation model of the nitrogen flow in the Peruvian upwelling system. Investigacion Pesquera 35, 309–330.

Ware, D.M., 1992. Production characteristics of upwelling systems and the trophodynamic role of hake. South African Journal of Marine Science 12, 501–514.

Ware, D.M., Thomson, R.E., 2005. Bottom-up ecosystem trophic dynamics determine fish production in the northeast Pacific. Science 308, 1280–1284.

Wilkerson, F.P., Dugdale, R.C., 1987. The use of large shipboard barrels and drifters to study the effects of coastal upwelling on phytoplankton nutrient dynamics. Limnology and Oceanography 32, 368–382.

Wilkerson, F.P., Dugdale, R.C., Marchi, A., Hogue, V., Lassiter, A., 2006. The phytoplankton bloom response to wind events and upwelled nutrients during the CoOP-WEST Study. Deep Sea Research II, submitted for publication.

Wroblewski, J., 1977. A model of phytoplankton plume formation during variable Oregon upwelling. Journal of Marine Research 35, 357–394.

Zimmerman, R.C., Kremer, J.N., Dugdale, R.C., 1987. Acceleration of nutrient uptake by phytoplankton in a coastal upwelling system: a modeling analysis. Limnology and Oceanography 32, 359–367.